

# High density helicon source for beam attenuating target

A. Okamoto, T. Isono, T. Nishiuchi, H. Takahashi, S. Kitajima and M. Sasao

*Department of Quantum Science and Energy Engineering, Tohoku University, Sendai 980-8579 Japan*

(Received: 19 November 2009 / Accepted: 5 February 2010)

High density ( $n_e \geq 4 \times 10^{18} \text{m}^{-3}$ ) helium plasma is produced in a linear device for the development of a neutral helium-beam attenuating target. Radially peaked density profile accompanied by one order of density jump is observed for radio frequency input power higher than the threshold power. The threshold power varies with the external magnetic field. The results suggest that the density jump is caused by the discharge transition from the inductively coupled mode to the helicon mode. Measurement of overall density profile for the axial direction shows the line integrated density is comparable to that required for the neutral helium-beam attenuating target.

Keywords: Helicon Discharge, Helium Plasma, Beam Attenuation, Helium Neutral Beam, Diagnostic Beam, Alpha Particle Diagnostics

## 1. Introduction

Neutral beams are key tools to probe the magnetically confined particles in fusion plasmas. For the measurement of the confined alpha particles in the International Thermonuclear fusion Experimental Reactor (ITER), an approximately 1–2 MeV helium neutral beam has been designed[1, 2, 3]. The diagnostic neutral beam is required to be well controlled regarding the population of helium atoms in the ground state. Since a neutral beam that includes considerable amount of metastable atoms causes undesired beam attenuation, quantitative evaluation of alpha particle distribution becomes difficult and measurement itself might be impossible near the magnetic axis.

In order to suppress production of the metastable state, a method using auto-detachment of negative helium ion ( $\text{He}^- \rightarrow \text{He}^0 + e$ ) has been proposed[4] and has been experimentally investigated using a laboratory-scale beam-test bench[5]. A high density-plasma target is required to attenuate the neutralized helium beam. The beam attenuation length then depends on a fraction of the metastable state and the ground state population in the beam. Therefore the target plasma assures production of the population controlled beam. In order to supply the target plasma, we have started to develop a high density helicon source. Helicon source has an advantage that high density plasma is produced under moderate gas-pressure and radio frequency (RF) input power[6, 7, 8, 9, 10, 11].

In our previous work, an argon plasma was investigated[12]. The plasma with the electron density of  $3.4 \times 10^{18} \text{m}^{-3}$  and the electron temperature of 10 eV was successfully produced. Helicon discharge was confirmed by rapid increase of the electron density and the magnetic field dependence of the electron density deduced from a dispersion relation. In our previous work also showed that required density for

the beam attenuation was  $n_e > 1 - 2 \times 10^{18} \text{m}^{-3}$  along 1–2 m length of plasma column. However, the required density should be achieved with helium plasma because of the advantages in the availability of abundant atomic data between the neutral helium beam and target plasma. In this paper, present achievement for production of a high density plasma using helium gas is described. Experimental setup is described in Sec. 2, the experimental results are shown in Sec. 3, followed by summary in Sec. 4.

## 2. Experimental Setup

The experiments were performed in a linear plasma device designed as a "Diagnostic Tool Assisted by Linear Plasma device for Helium Atom beam (DT-ALPHA)" [12]. A schematic of the experimental setup is shown in Fig. 1. The vacuum chamber consists of a quartz pipe (0.4 m in length, 36 mm in inner diameter) coupling an antenna to a plasma, and a main chamber (1.1 m in length, 63 mm in inner diameter) made of stainless steel. An end-plate with an aperture (10 mm in inner diameter) made of stainless steel is equipped at the entrance of the quartz pipe,  $z = 0.3$  m, where  $z$  is the axial coordinate.

Helium gas is fed with a flow rate of  $0.17 \text{Pa m}^3/\text{s}$  from an end of the quartz pipe. Turbo molecular pumps (TMPs) are equipped at upstream and downstream manifolds. Only the upstream TMP is used for a high pressure operation, then working gas pressure  $p = 2.3$  Pa is sustained throughout the main chamber and the quartz pipe. On the other hand, both TMPs are used for a low pressure operation, then the pressure measured at the downstream manifold is  $p = 0.17$  Pa. Due to the gas conductance, the working pressure in the main chamber and in the quartz pipe are about three to ten times higher than that measured at the downstream manifold for the low pressure operation.

A flat magnetic field is applied along the axial direction. Magnetic field intensity is  $B = 0.08 - 0.14$  T

author's e-mail: atsushi.okamoto@qse.tohoku.ac.jp

in the present experiment. A so-called Nagoya type III antenna[13] ( $l = 0.15$  m) is used to produce the plasma, which is connected to a 13.56 MHz RF oscillator through a matching circuit.

Plasma parameters are evaluated using the current ( $I$ )-voltage ( $V$ ) characteristics of radially movable double probes installed at  $z = 1, 1.3, 1.6$  m, an axially movable single Langmuir probe ( $z = 0.14 - 0.37$  m). Passive spectroscopy is also applied. Emission of the plasma is collected by axially movable optics and is transferred to a spectrograph.

Atomic helium lines (He I), 667.8 nm ( $2^1P - 3^1D$ ) and 726.1 nm ( $2^1P - 3^1S$ ), are measured to obtain the electron density. The line intensity ratio measured by the experiment is compared to that obtained by a collisional radiative model [14, 15]. The line intensity ratio varies with electron density but is insensitive to the electron temperature[16].

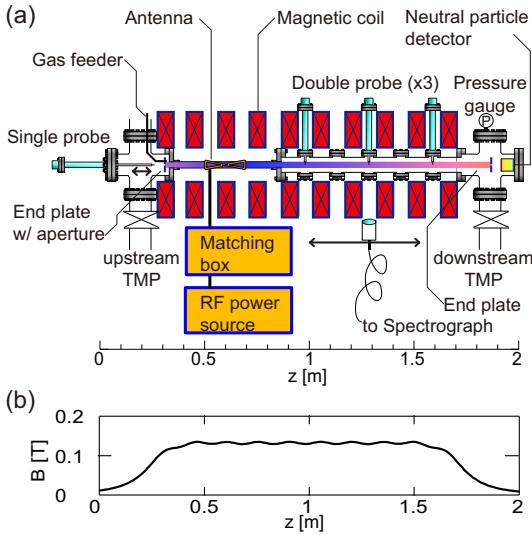


Fig. 1 (a) Schematic of the experimental setup and (b) typical magnetic field configuration of DT-ALPHA device.

### 3. Results and discussion

#### 3.1 production of high density plasma

RF power dependence of electron density and temperature was investigated using a double probe at  $z = 1$  m. The electron density increases with RF power; up to  $n_e \geq 4 \times 10^{18} \text{m}^{-3}$  is obtained for  $P_{\text{RF}} > 500$  W of input power as shown in Fig. 2(a). 'Density jumps' with more than one order of rapid increase of electron density are observed. The electron density after the density jump is comparable to that obtained using argon gas in this device[12]. The threshold power of the density jump decreases from  $P_{\text{RF}} = 1.2$  kW to 300 W, when the external magnetic field increases from  $B = 0.082$  T to 0.14 T. The electron temperature also shows rapid change but de-

creases to about 5 eV at the threshold power of the density jump as shown in Fig. 2(b).

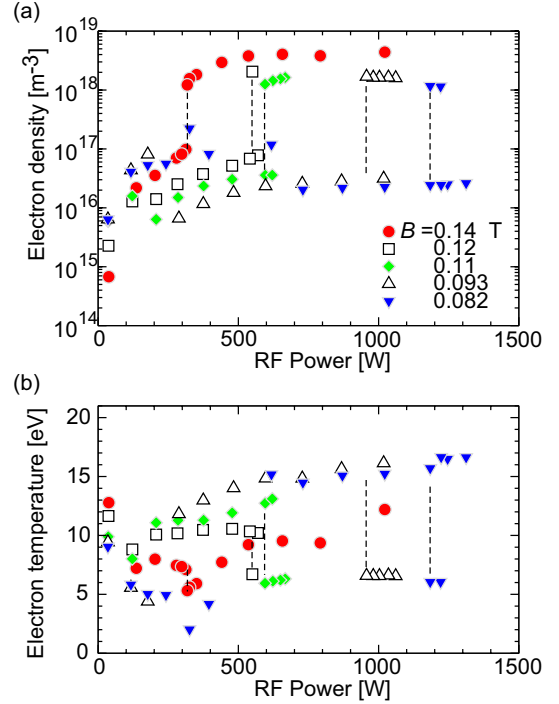


Fig. 2 RF power dependence of (a) electron density and (b) temperature at  $r = 0, z = 1$  m. Vertical dashed lines show density jump. Helium gas,  $p = 2.3$  Pa is used.

The electron density is plotted as a function of the magnetic field in Fig. 3. The filled symbols in the figure indicate the experimental data, where gaps observed around  $10^{17} < n_e < 10^{18} \text{m}^{-3}$  indicate the density jump. The dispersion relation of a plane wave in a cold uniform plasma is calculated. That for the minimum wave number ( $k_z = 0.021 \text{cm}^{-1}$ ) in the parallel direction is also plotted in Fig. 3, in which the half wavelength corresponds to the distance between the end-plates. Perpendicular wave number  $k_{\perp} = 0.6 - 1.3 \text{cm}^{-1}$  corresponds to wavelength of the order of the chamber radius. Thus the dispersion curve in Fig. 3 indicates whether the helicon wave could propagate or not. The experimental data over the density jump are matched with the dispersion relation of the helicon wave. Thus, the density jump suggests the discharge transition from the inductively coupled mode to the helicon mode. Open symbols in Fig. 3, which are obtained in a low pressure ( $p = 0.17$  Pa) operation, imply that the helicon plasma is also produced even in the low pressure helium gas.

#### 3.2 target plasma for beam attenuation

In terms of the beam injection experiment, lower gas pressure operation is preferable. Thus, spatial profile of a low gas-pressure plasma was investigated.

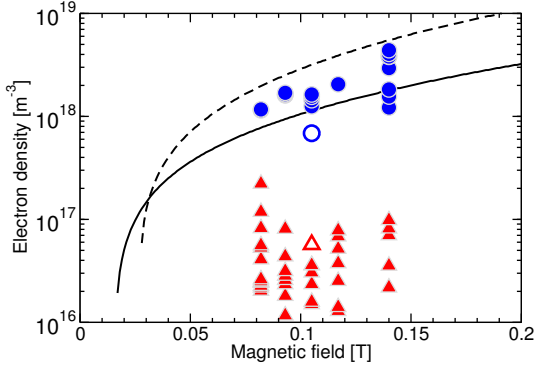


Fig. 3 Magnetic field dependence of electron density measured at  $r = 0$ ,  $z = 1$  m. Filled symbol corresponds to experimental data in  $p = 2.3$  Pa with various RF power, open symbol in  $p = 0.17$  Pa. Circle and triangle represent helicon- and inductively coupled discharge, respectively. Solid and dashed curve indicate dispersion relation of a plane wave in a cold uniform plasma, where  $(k_{\parallel}, k_{\perp}) = (0.021 \text{ cm}^{-1}, 0.6 \text{ cm}^{-1})$  for solid curve and  $(0.021 \text{ cm}^{-1}, 1.3 \text{ cm}^{-1})$  for dashed curve are used for calculation.

Radial profiles of the electron density and temperature measured in helium gas pressure  $p = 0.17$  Pa are shown in Fig. 4(a) and (b). A hollow density profile due to the inductively coupled production is observed for low power ( $P_{\text{RF}} = 570$  W) operation. Position of the density peaks corresponds to inner radius of the quartz pipe; the plasma production by the near field of the RF antenna is a possible reason. The radial density profile changes to peaked one, when RF input power exceeds the threshold power of the density jump. The peak density reaches up to  $0.67 \pm 0.01 \times 10^{18} \text{ m}^{-3}$  with the plasma radius about 10 mm in full width at half maximum. The profile contrasts to that for the inductively coupled plasma, and is similar to that obtained in an argon plasma[12]. The electron density reaches  $0.6 \times 10^{18} \text{ m}^{-3}$  within radius  $r \leq 5$  mm, the beam radius injected through the aperture, which is acceptable value for the beam injection target. In contrast to the density profile, the temperature profile changes from peaked one to flat one.

In order to evaluate the line integrated density along the beam path, measurement of density profile was performed by three probes installed at  $z = 1, 1.3, 1.6$  m. Radial density profiles were similar among them, while maximum density gradually decreased apart from the antenna ( $z = 0.6$  m) as shown in Fig. 5. One order higher density is sustained in wide region, at least  $z = 1 - 1.6$  m, for high power ( $P_{\text{RF}} = 870$  W) operation than that for low power ( $P_{\text{RF}} = 570$  W) operation. Spectroscopic measurement for the high power operation also shows that the

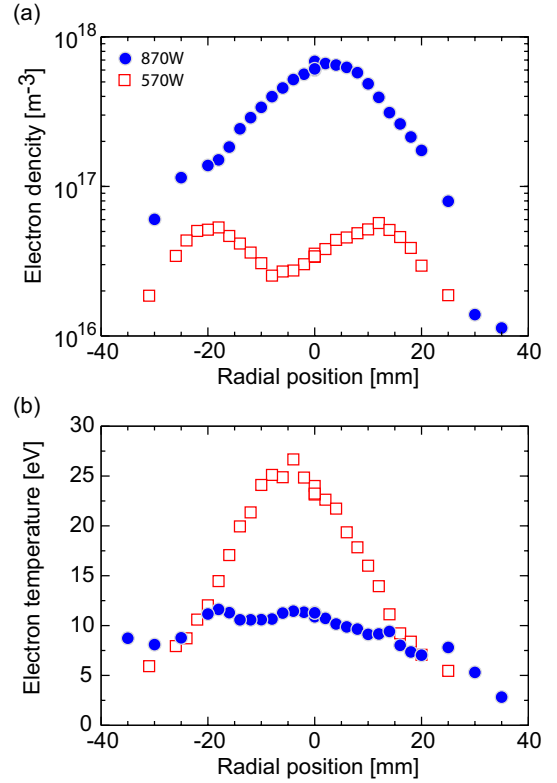


Fig. 4 Radial distribution of electron density and temperature measured at  $r = 0$ ,  $z = 1$  m. Closed circle for high density mode ( $P_{\text{RF}} = 870$ W), open square for low density mode ( $P_{\text{RF}} = 570$ W). Magnetic field and working pressure are  $B = 0.11$  T and  $p = 0.17$  Pa, respectively.

chamber is filled by high density plasma.

On the other hand, the electron density rapidly decreases at the beam entrance aperture ( $z = 0.3$  m). Thus, the effect of plasma leaking from the aperture on collision with the injected beam is negligibly-small. Rapid decreasing from  $3 \times 10^{17} \text{ m}^{-3}$  ( $z = 0.34$  m) to  $4 \times 10^{16} \text{ m}^{-3}$  ( $z = 0.30$ ) exists in front of the entrance aperture toward the entrance aperture implying the presheath structure. The divergent magnetic field and extremely low gas-pressure due to differential pumping can also contribute the rapidly decreasing density profile, especially outside of the aperture ( $z < 0.3$  m).

Line integrated density is deduced from the axial density profile. Since the electron density measured by the single probe (diamond in Fig. 5) is about five times lower than that measured by the spectroscopy (square) at  $z = 0.4$  m, we expect that true density is within those densities. Using linear interpolation between experimental data, line integrated density of the helium plasma  $0.5 - 1 \times 10^{18} \text{ m}^{-2}$  is obtained, where the range of the line integrated density corresponds to lower and upper envelope of the density profile. The line integrated density for the helium discharge

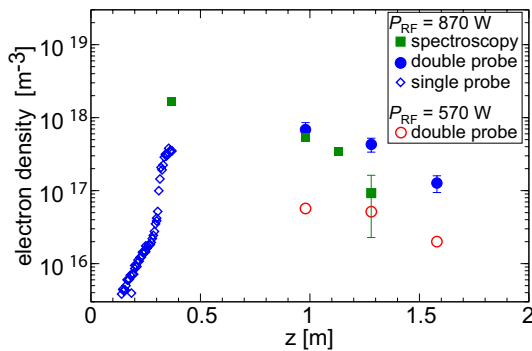


Fig. 5 Axial distribution of electron density measured by spectroscopy assuming  $T_e = 10$  eV (filled square), double probes ( $P_{\text{RF}} = 870$  W, filled circle), double probes ( $P_{\text{RF}} = 570$  W, open circle), and a single probe (open diamond). RF input power for spectroscopy and single probe is  $P_{\text{RF}} = 870$  W. Error bar in spectroscopy shows electron temperature variation  $T_e = 5 - 20$  eV. Magnetic field and working pressure are  $B = 0.11$  T and  $p = 0.17$  Pa, respectively.

is about 20–30% of that for an argon plasma[12] and is comparable to that required for the neutral helium beam attenuation target. However, since the ionization degree is of the order of one percent, interactions between the beam and the residual gas should be considered. Evaluation of the neutral density profile along the axis is significant as well as development of higher density-plasma production method in lower pressure operation.

For higher density-plasma production, magnetic configuration near the antenna is a possible control knob. While flat magnetic field is applied in the present experiment, a converging magnetic field[17] would increase the electron density far from the antenna. Optimization of the magnetic field configuration remains our future work.

#### 4. Summary

We have produced high density helicon plasma using helium in the DT-ALPHA device. Radially peaked density profile accompanied by one order of density jump are observed for RF power higher than a threshold. Relation between the external magnetic field and electron density is experimentally obtained and is compared to that derived from a dispersion relation. The result suggests that the density jump is caused by the discharge transition from the inductively coupled mode to the helicon mode. Those results obtained using helium gas have similar feature to that obtained using argon gas. Moreover, measurement of overall density profile for axial direction shows line integrated density almost is comparable to that required for the neutral helium beam attenuation target.

#### Acknowledgements

This work was partly supported by the Ministry of Education, Culture, Sports, Science and Technology of Japan (MEXT) Grant-in-Aid for "Priority area of Advanced Burning Plasma Diagnostics" (16082201).

- [1] M. Sasao, A. Taniike, I. Nomura, M. Wada, H. Yamaoka, and M. Sato, *Nucl. Fusion* **35**, 1619 (1995).
- [2] K. Shinto, A. Okamoto, S. Kitajima, M. Sasao, M. Nishiura, O. Kaneko, S. Kiyama, H. Sakakita, Y. Hirano, and M. Wada, *In Proceedings of EPAC 2006, Edinburgh, Scotland* 1726 (2006).
- [3] M. Sasao, K. Shinto, M. Isobe, M. Nishiura, O. Kaneko, M. Wada, C.I. Walker, S. Kitajima, A. Okamoto, H. Sugawara, S. Takeuchi, N. Tanaka, H. Aoyama and M. Kasaki, *Rev. Sci. Instrum.* **77**, 10F130 (2006).
- [4] M. Sasao and K.N. Sato, *Fusion Technol.* **10**, 236 (1986).
- [5] N. Tanaka, H. Sugawara, S. Takeuchi, S. Asakawa, A. Okamoto, K. Shinto, S. Kitajima, M. Sasao, and M. Wada, *Plasma Fusion Res.* **2**, S1105 (2007).
- [6] R.W. Boswell, *Plasma Phys. Control. Fusion* **26**, 1147 (1984).
- [7] T. Shoji, Y. Sakawa, S. Nakazawa, K. Kadota, and T. Sato, *Plasma Sources Sci. Technol.* **2**, 5 (1993).
- [8] S. Shinohara, Y. Miyauchi, and Y. Kawai, *Plasma Phys. Control. Fusion* **37**, 1015 (1995).
- [9] F.F. Chen, *Phys. Plasmas* **3**, 1783 (1996).
- [10] Y. Sakawa, T. Takino, and T. Shoji, *Phys. Plasmas* **6**, 4759 (1999).
- [11] K. Takahashi, C. Charles, R. Boswell, and R. Hatakeyama *Phys. Plasmas* **15**, 074505 (2008).
- [12] A. Okamoto, K. Iwazaki, T. Isono, T. Kobuchi, S. Kitajima, and M. Sasao *Plasma Fusion Res.* **3**, 059 (2008).
- [13] T. Watari, T. Hatori, R. Kumazawa, S. Hidekuma, T. Aoki, T. Kawamoto, M. Inutake, S. Hiroe, A. Nishizawa, K. Adati, T. Sato, T. Watanabe, H. Obayashi, and K. Takayama, *Phys. Fluids* **21**, 2076 (1978).
- [14] M. Goto, *J. Quant. Spectrosc. Radiat. Transf.* **76**, 331 (2003).
- [15] T. Fujimoto, *J. Quant. Spectrosc. Radiat. Transf.* **21**, 439 (1979).
- [16] B. Schweer, G. Mank, A. Pospieszczyk, B. Brosda, B. Pohlmeier, *J. Nucl. Mater.* **196-198**, 174 (1992).
- [17] V.F. Virko, K.P. Shamrai, Yu.V. Virko, G.S. Kirichenko, *Phys. Plasmas* **15**, 084501 (2004).